J M M
Journal of Mechanics and MEMS
Special Issue dedicated to Prof. K Y Ye edited by Z M Ye, P Liu and B Sun

ISSN: 0974-8407

9(2) 2017: pp. 287-298

ON THE NONLINEAR MECHANICAL BEHAVIOUR OF CIRCULAR DIELECTRIC ELASTOMER FILMS UNDER LARGE DEFORMATION

X. D. Wang[1] and J. W. Zu[2]

ABSTRACT

This paper presents a comprehensive theoretical study of the large deflection of pre-strained circular dielectric elastomer films with a rigid boundary subjected to electric and mechanical loads. Both material and geometric nonlinearity of the films are included in the formulation of the problem and a set of nonlinear differential equations are established. The resulting governing equations are solved numerically using an iteration process to study the nonlinear response of the films. Special attention is focussed on the instability and the multi-mode behaviour of the films under different electromechanical loads and pre-strain conditions. The conditions under which the films become instable is discussed and the multi-modes of the films are presented for typical loading conditions.

1. INTRODUCTION

Dielectric elastomers are capable of generating large deformations by transforming electric energy directly into mechanical energy. For this superior feature, dielectric elastomers are now being considered for use in the design of new actuator systems, such as microrobots, micropumps, microvalves and prosthetic devices [Wissler and Mazza, 2005; Zhang *et al.*, 2005; Pelrine *et al.*, 2000a], to name a few. A recent application of dielectric elastomers is for prosthetic blood pumps [Goulbourne *et al.*, 2005]. Such a device is made from a circular dielectric elastomer actuator consisting of a compliant capacitor, which is a thin passive elastomer film sandwiched between two compliant electrodes. When an electric voltage is applied between the electrodes, an electrostatic field is generated and the electrostatic force mechanically loads the polymer film. As a result, the film contracts in the direction of thickness and expands in the plane of the film. Due to the complexity of high nonlinearity and electromechanically coupling, understanding of the electromechanical behaviour of dielectric elastomer elements is limited. To facilitate the design of dielectric elastomer actuators, it is important to develop suitable modelling techniques to deal with the complicated properties of the actuators.

The mechanical behaviour of thin films subjecting to transverse loads has been extensively studied [Adkins and Rivlin, 1952; Szyszkowski and Glockner, 1984; Duan *et al.*, 2004; Komaragiri, 2005]. For dielectric elastomer thin films, electromechanical coupling must be considered. The electromechanical coupling in a dielectric elastomer element is mainly caused by the electrostatic Coulomb forces between electrodes [Jackson, 1962]. To focus on the mechanism of electromechanical coupling due to electrostatic forces, the insignificant electrostrictive [Pelrine *et al.*, 1998; Wolfson and Pasachoff, 1999] and piezoelectric [Parton and Kudryavtsev, 1988, Wang, 1999; Wang and Meguid, 2000; Giurgiutiu *et al.*, 2002] effects should be ignored. Goulbourne *et al.* (2005) studied the large deformation of circular dielectric elastomer films and presented the variation of deformation of the films with applied electric and mechanical loads. Their work was focused on the stable deformation of the films and they demonstrated that dielectric elastomer films can be effectively used as active elements. However, as mentioned by Adkins and Rivlin (1952), a thin film subjected to an applied external pressure may experience a pressure drop with increasing deformation, indicating the existence of instability.

1. Department of Mechanical Engineering, University of Alberta, Edmonton, Alberta, Canada
2. Department of Mechanical and Industrial Engineering, University of Toronto, Toronto, Ontario, Canada

Since dielectric elastomer actuators usually work under very large strain, the property of elastomer films is governed by both material and geometric nonlinearities. Two important issues arise from such nonlinear problems. First, since the elastomer films are almost incompressible [Wissler and Mazza, 2005], significant reduction of the thickness will occur under large inplane deformation. This thickness reduction may result in a significant increase in the Cauchy stresses along the films, which in turn will increase the deformation of films. For certain material properties and loading conditions, a stable deformation may be established and for other cases this process may continue until instability occurs. Since actuators of this type are working mostly under large deformation, the condition under which instability occurs should be carefully investigated. Second, because of the material and geometric nonlinearity, elastomer films subjected to a specific electromechanical load may reach equilibrium at different final geometries and result in multiple deformation modes. This is another important issue for the evaluation of the electromechanical behaviour of elastomer films under large deformation. Unfortunately, understanding of the unstable behaviour of dielectric elastomer films under electromechanical loads is very limited at present.

To fully understand the nonlinear behaviour of dielectric elastomer films, this paper presents a comprehensive study of dielectric elastomer films subjected to applied electric voltage and transverse pressure. Large rotation of the films is included in the formulation of the problem and a set of differential equations are established. The solution of these equations is obtained by using an iteration process. The instability and the multi-mode behaviour are studied for circular dielectric elastomer films under different loading and prestrain conditions. The effects of geometry, pre-strain and applied loads upon the stable nonlinear behaviour of the films are also studied. The condition under which the films become unstable is discussed and the multi-modes of the films are presented for typical loading conditions.

2. STATEMENT AND FORMULATION OF THE PROBLEM

Consider a circular dielectric elastomer film with initial thickness H and radius R_0. A cylindrical coordinate system (r, w) is used to describe the deformed geometry of the axis-symmetric problem, as shown in Figure 1 with r representing the position of a point in the radial direction in the deformed geometry, and w representing the deflection of the film at that point. The film is pre-stretched with a stretch ratio λ_0, and is fixed along a circular rigid boundary, $r = R_0 \lambda_0$. It is assumed that two electrodes are attached to the two surfaces of the film [Pelrine *et al.*, 2000b], respectively, and an electric voltage is applied across the electrodes. A pressure p is also applied, which is assumed to be always perpendicular to the film, to simulate fluid pressure in dielectric elastomer pumps.

2.1. Material Property

The dielectric elastomer considered is assumed to be hyperelastic. The time dependance of the material property is ignored and the material is assumed to be incompressible, isotropic and homogeneous in the undeformed configuration. Three typical constitutive relations for hyperelastic materials by Mooney-Rivlin [1940], Ogden [1972]

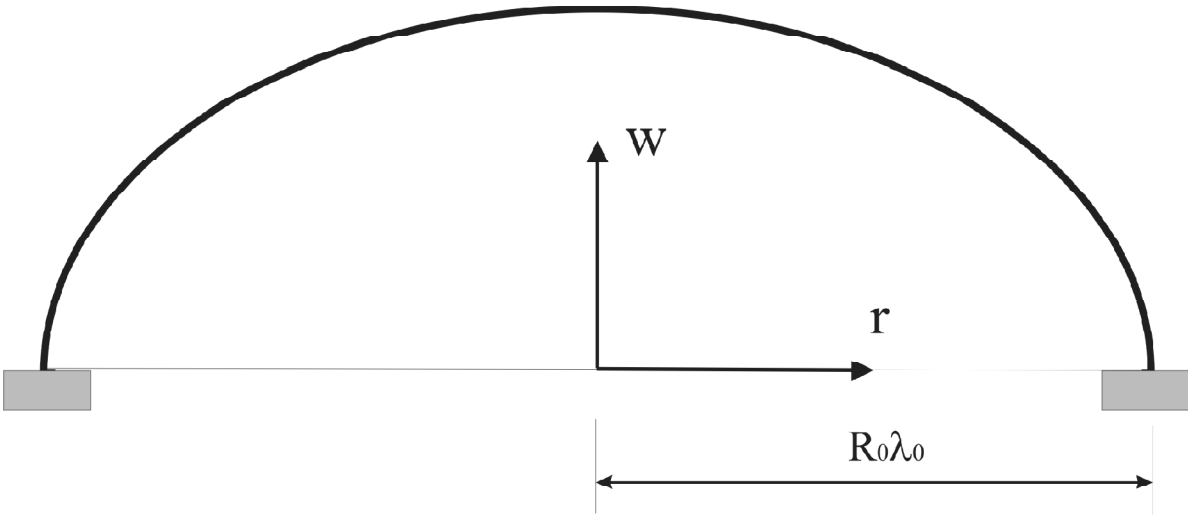

Figure 1: Deformed Geometry of a Dielectric Film

and Yeoh [1993] can be used to describe the mechanical property of hyperelastic material. Theoretical and experimental studies [Wissler and Mazza, 2005] indicate that for the simple uniaxial tension case all three models agree very well with the experimental results for stretch ratios at least up to five. For the biaxial loading case Ogden and Yeoh models also show consistent results for stretch ratios up to five, which are different from that of the Mooney-Rivlin model. It has been suggested that Ogden model is suitable for dielectric elastomer materials [Wissler and Mazza, 2005; Goulbourne *et al.*, 2005]. In the current study, the Ogden's model is used for simulating the material property of dielectric elastomers.

In Ogden's model, the strain energy function U is represented in terms of the principal stretch ratios, such that

$$U = \sum_{k=1}^{M} \frac{\mu_k}{\alpha_k} \left(\lambda_1^{\alpha_k} + \lambda_2^{\alpha_k} + \lambda_3^{\alpha_k} - 3 \right) \tag{1}$$

where λ_1, λ_2, λ_3 are the three principle stretch ratios, μ_k, α_k are material constants, and M is the number of terms. For incompressible materials, the following relation also exists,

$$\lambda_1 \lambda_2 \lambda_3 = 1 \tag{2}$$

The principle Cauchy stress t_i (force per unit area of the deformed configuration) can be obtained by

$$\sigma_i = \lambda_i \frac{\partial U}{\partial \lambda_i} - \bar{p} \tag{3}$$

with $\bar{p}$ being a hydrostatic pressure, which is arbitrary for the constitutive equation (3) and must be determined from the boundary conditions.

For the currently considered dielectric elastomer film, the applied electric field will generate an electrostatic pressure p_{el} across the electrodes attached to the two sides of it [Anderson, R. A., 1986; Pelrine *et al.*, 1998],

$$q = \epsilon_r \epsilon_0 \left(\frac{U}{h} \right)^2 \tag{4}$$

which results in a Cauchy stress in the thickness direction. If axial-3 is assumed parallel to the thickness direction, this stress component can be expressed as

$$\sigma_3 = -q = -\epsilon_r \epsilon_0 \left(\frac{U}{h} \right)^2 \tag{5}$$

From (3) and (5), the constitutive equations of the hyperelastic material can be expressed as,

$$\sigma_1 = \sum_{k=1}^{M} \mu_k \left[\lambda_1^{\alpha_k} - (\lambda_1 \lambda_2)^{-\alpha_k} \right] - \epsilon_r \epsilon_0 \left(\frac{U}{h} \right)^2 \tag{6}$$

$$\sigma_2 = \sum_{k=1}^{M} \mu_k \left[\lambda_2^{\alpha_k} - (\lambda_1 \lambda_2)^{-\alpha_k} \right] - \epsilon_r \epsilon_0 \left(\frac{U}{h} \right)^2 \tag{7}$$

$$\sigma_3 = -\epsilon_r \epsilon_0 \left(\frac{U}{h} \right)^2 \tag{8}$$

2.2. Formulation of the Dielectric Films

The dielectric elastomer films considered will usually undergo very large deflection. Under the assumption that the thicknesses of the films are much smaller than the radii of the curvatures, the films can be simplified as membranes.

The final configuration of the middle surface of the film can be described as

$$w = w(r) \tag{9}$$

where w is the deflection and r is the position of the point initially located at R, with

$$R = R(r) \tag{10}$$

The stretch ratios of the membrane in the longitudinal, latitudinal and transverse directions are given by [Adkins and Rivlin, 1952]

$$\lambda_1 = \frac{ds}{dR},\ \lambda_2 = \frac{r}{R},\ \lambda_3 = \frac{1}{\lambda_1\lambda_2} \tag{11}$$

with s being the meridian curve length in the deformed configuration. λ_1 can also be expressed in terms of w and r as

$$\lambda_1 = \sqrt{1+\left(\frac{dw}{dr}\right)^2}\Big/\frac{dR}{dr}. \tag{12}$$

The radii of curvatures of the membranes in the principle directions, ρ_1 and ρ_2, can be determined in terms of w and r as

$$\rho_1^{-1} = -\frac{d^2w}{dr^2}\Big/\left(1+\left(\frac{dw}{dr}\right)^2\right)^{3/2} \tag{13}$$

$$\rho_2^{-1} = -\frac{1}{r}\frac{dw}{dr}\Big/\left(1+\left(\frac{dw}{dr}\right)^2\right)^{1/2} \tag{14}$$

The equilibrium equations of the membranes in the deformed geometry can be expressed in terms of the longitudinal and latitude forces, N_1 and N_2, as

$$\frac{N_1 - N_2}{r} + \frac{dN_1}{dr} = 0 \tag{15}$$

$$\frac{N_1}{\rho_1} + \frac{N_2}{\rho_2} - p = 0 \tag{16}$$

where

$$N_1 = h\sigma_1 = H\lambda_3\sigma_1;\ \ N_2 = h\sigma_2 = H\lambda_3\sigma_2 \tag{17}$$

with h being the thickness of the deformed films,

$$h = H\lambda_3 = \frac{H}{\lambda_1\lambda_2}. \tag{18}$$

Substituting the constitutive equations (6) and (7), the geometric conditions (13) and (14) and (17), (18) into equilibrium equations (15) and (16), the following governing equations can be obtained,

$$(F_1 - \lambda_1\lambda_2^2 q)\frac{d\lambda_1}{dr} + (F_2 - \lambda_1^2\lambda_2 q)\frac{R - r\frac{dR}{dr}}{R^2} + F_5 = 0 \tag{19}$$

and

$$\frac{p\lambda_1\lambda_2}{h\mu_1} + \frac{\frac{d^2w}{dr}}{\left(1+\left(\frac{dw}{dr}\right)^2\right)^{3/2}}F_3 + \frac{1}{\left(1+\left(\frac{dw}{dr}\right)^2\right)^{3/2}}F_4 = 0 \tag{20}$$

where

$$F_1 = \sum_{k=1}^{M} \mu_k [(\alpha_k - 1)\lambda_1^{\alpha_{k-1}} + (\alpha_k + 1)\lambda_1^{-\alpha_{k-1}} \lambda_2^{-\alpha_k}$$

$$F_2 = \sum_{k=1}^{M} \mu_k [-\lambda_1^{\alpha_k} \lambda_2^{-1} + (\alpha_k + 1)\lambda_2^{-\alpha_k - 1} \lambda_1^{-\alpha_k}]$$

$$F_3 = \sum_{k=1}^{M} \mu_k [\lambda_1^{\alpha_k} - (\lambda_1 \lambda_2)^{-\alpha_k}] \tag{21}$$

$$F_4 = \sum_{k=1}^{M} \mu_k [\lambda_2^{\alpha_k} - (\lambda_1 \lambda_2)^{-\alpha_k}]$$

$$F_5 = \sum_{k=1}^{M} \frac{\mu_k}{r} (\lambda_1^{\alpha_k} - \lambda_2^{\alpha_k})$$

In addition, the following boundary conditions must be satisfied,

$$\begin{aligned} &R = 0, \quad \frac{dw}{dr} = 0, \quad \textit{when } r = 0 \\ &w = 0, \quad \lambda_2 = \lambda_0, \quad \textit{when } r = R_0 \lambda_0 \end{aligned} \tag{22}$$

The nonlinear equations, (19) and (20), are difficult to solve even numerically. To overcome the difficulties, the step-by-step integration of the equations will be performed and an iteration process will be used to solve the problem. To complete the integration, the behaviour of the equations when $r \to 0$ needs to be carefully evaluated. Since $\lambda_2 = r = R$, when $r \to 0$ it can be obtained that $\lambda_2 \lambda$ 1/$R'(0)$. Because $\lambda_1 = \sqrt{1 + (dw/dr)^2} / \dfrac{dR}{dr}$ and $dw = dr = 0$ when $r = 0$, $\lambda_1 \to 1 / R'(0)$ when $r \to 0$. Therefore, $\lambda_1 = \lambda_2$ at $r = 0$.

Evaluating the limit of $(R - rR') = R^2$ when $r \to 0$ indicates that $(R - rR') = R^2 \to -R''(0) = [R'(0)]^2$. From equation (12), $\lambda_1' = w'w''/[R'\sqrt{1 + (w')^2}] - \sqrt{1 + (w')^2} R''/(R')^2$. When $r \to 0$, $w' \to 0$ and, therefore, $\lambda_1' \to -R''/(R')^2$.. Thus when $r \to 0$, $\lambda_1' = \lambda_2'$.

Based on these relations, the integration can be carried out and the following iteration process is used to get the numerical solution. First the stretch ratio λ_1 at $r = 0$ (equals to λ_2) is assumed. Equations (19) and (20) can then be integrated based on the boundary conditions at $r = 0$ from $r = 0$ to $r = R_0 \lambda_0$ to give the distribution of $\lambda_1(r)$, $\lambda_2(r)$, $w(r)$ and $R(r)$. The boundary condition $R = R_0$ will then be checked at $r = R_0 \lambda_0$ and a renewed value of the stretch ratio λ_1 at $r = 0$ will be used in the next integration from $r = 0$ to $r = R_0 \lambda_0$. This iteration process will be repeated until a convergent result is achieved. It should be mentioned that the value of w at $r = 0$ can be arbitrarily selected for the iteration since it will not affect the integration process. When the convergent solution is obtained the value of w at $r = R_0 \lambda_0$ is set to be zero and w values at other positions are shifted correspondingly to give the final solution of the problem.

The solution is used to study the nonlinear behaviour of dielectric elastomer films. Attention will first be focussed on the instability of the films under inplane electromechanical loading. The instability of the films under large transverse deformation will then be discussed.

3. INSTABILITY OF THE FILMS UNDER INPLANE ELECTROMECHANICAL LOADS

Consider a dielectric elastomer film subjected to an applied voltage V across the electrodes attached to its two surfaces. Forces are also applied along 1 and 2 directions, which result in initial stresses σ_1^0, σ_2^0 in the underformed

configuration. The stresses caused by these forces in the deformed configuration can be determined by using the incompressible condition of the film as

$$\sigma_1 = \sigma_1^0 \lambda_1, \ \sigma_2 = \sigma_2^0 \lambda_2 \tag{23}$$

$$\sigma_3 = -\epsilon_r \epsilon_0 \left(\frac{V}{H}\right)^2 \frac{1}{\lambda_3^2}. \tag{24}$$

For the current incompressible film, with the increase of the stretch ratios λ_1 and λ_2 caused by the applied loads, the thickness and the area of the cross-section will decrease to keep the volume unchanged. This will result in the increase of the Cauchy stress components, σ_1, σ_2 and σ_3, even if the applied loads are kept to be constants. Obviously, this will further increase the deformation and result in higher stress. It is, therefore, possible to result in an unstable process, similar to the tensile instability in the simple tension of metals.

To study the deformation stability of the dielectric elastomer films, rewrite the constitutive relations (6), (7) and (24) as

$$\sigma_1^0 \lambda_1 + \frac{q}{\lambda_3^2} = f(\lambda_1, \lambda_2) \tag{25}$$

$$\sigma_2^0 \lambda_2 + \frac{q}{\lambda_3^2} = f(\lambda_2, \lambda_1)$$

$$\sigma_3 = -\frac{q}{\lambda_3^2}$$

with

$$f(\lambda_1, \lambda_2) = \sum_{k=1}^{M} \mu_k [\lambda_1^{\alpha_k} - (\lambda_1 \lambda_2)^{-\alpha_k}] \tag{26}$$

and q being given by equation (4), representing the stress due to the applied electric voltage in the undeformed geometry.

Case 1 Electric Instability with Constant Forces

When constant forces, which resulting in $\sigma = \sigma_1^0 = \sigma_2^0$, are applied, $\lambda_1 = \lambda_2$ and

$$q = \frac{1}{\lambda_1^4} F(\lambda_1) - \frac{\sigma}{\lambda_3} \tag{27}$$

with

$$F(\lambda_1) = f(\lambda_1, \lambda_1). \tag{28}$$

When $\frac{dQ}{d\lambda_1} < 0,$ instability occurs, which corresponds to

$$F'(\lambda_1) < 4F(\lambda_1) = \lambda_1 - 3\sigma \tag{29}$$

Case 2 Tensile Instability with a Constant Voltage

Assuming that the applied forces are given by $\sigma = \sigma_1^0 = \sigma_2^0$. It follows that $\lambda_1 = \lambda_2$, and

$$\sigma = \frac{1}{\lambda_1} F(\lambda_1) - \lambda_1^3 q. \tag{30}$$

When $\frac{d\sigma}{d\lambda_1} < 0,$ instability occurs, which corresponds to

$$F'(\lambda_1) < F(\lambda_1) = \lambda_1 + 3\,\lambda^3 q. \tag{31}$$

These equations predict that the instability condition of the films under in-plane deformation depends on the material property and the loading condition.

For case 1, if no force is applied, i.e. $\sigma = 0$, then equation (29) becomes

$$\frac{F'(\lambda_1}{F(\lambda_1)/\lambda_1} < 4. \tag{32}$$

For hyperelastic materials governed by the Ordgen's model, as described by (6) and (7), $F' = (F = \lambda_1)$ approaches α_1 when λ_1 approaches infinity, assuming that $\alpha_j < \alpha_1$ when $j > 1$. Therefore, the instability condition will be satisfied if $\alpha_1 < 4$. For case 2, if no electric field is applied, equation (31) becomes

$$\frac{F'(\lambda_1}{F(\lambda_1)/\lambda_1} < 1. \tag{33}$$

Figure (2) shows the value of $\frac{F'(\lambda_1}{F(\lambda_1)/\lambda_1}$ for different α_1 based on the Ordgen's model with only the first term considered, i.e. $mu_k = 0$ in equations (6) and (7) for $k > 1$. It can be observed that for α_1 values smaller than 4.0, the instability due to the electric field, determined by (32), can always be achieved. For example, for $\alpha_1 = 1$, 2 and 3, instability occurs at about $\lambda_1 = 1{:}25$. The tensile loads will not result in insability unless $\alpha_1 < 1$, which does not represents reasonable material constants for existing dielectric elastomers.

4. THE PROPERTY OF THE MEMBRANE UNDER ELECTROMECHANICAL LOADS

For dielectric elastomer films subjected to applied external pressure and electric voltage, their nonlinear response can be determined by solving equations (19) and (20) numerically using an iteration process as discussed before.

The material used for the current dielectric film is an acrylic polymer, VHB 4910 (3M), which has the following material constants [Wissler and Mazza, 2004],

$$\alpha_1 = 1{:}76, \quad \mu_1 = 0{:}156 Mpa \tag{34}$$

Large Deformation of the Films

This subsection presents the effect of pertinent parameters upon the large deformation of the film under different electromechanical loads.

Figure 3 shows the final shape of a dielectric film under different applied pressures with no electric voltage being applied. The thickness and initial radius of the film are $H = 1mm$ and $R_0 = 50mm$. The film is pre-strained with a stretch ratio $\lambda_0 = 2.0$. As expected, an increase in the deflection of the film with increasing pressure is observed. A maximum deflection of $8cm$ at the centre of the film is achieved at a pressure of $2537pa$. This pressure value happens to be the critical pressure for this film, which will be discussed later. Figure 4 shows the results when an electric field, resulting in an electric force $q = 2000pa$, is applied. The results in figure 4 are similar to that given in figure 3 with $p = 2167$ being the critical pressure. But a higher deflection is observed for the same applied pressure. The highest pressure at which the film will stay stable is reduced significantly due to the existence of the electric field.

The displacement of the film in the radial direction under only the pressure is presented in figure 5. It is interesting to see that the relation between the initial position of a point R and its final position r is almost linear for most loading levels, except for the case where the pressure approaches the critical value. Similar property can be observed when both electric voltage and pressure are applied, as shown in figure 6, with $Q = 2000pa$.

The distributions of the stretch ratio and the stress in the film are interesting to the understanding of the deformation of the film. Figure 7 shows the stretch ratios of a film with a thickness of $5mm$ subjected to a pressure of $15000pa$. The corresponding results of the film subjected to an additional electric voltage with $q = 8000pa$ is given in figure 8. The initial stretch ratio of the film is assumed to be 1.2 in both cases. Maximum stretch ratios (λ_1 and λ_2) occur at $r = 0$ for all the loading cases. Figures 9 and 10 show the corresponding stresses and forces in the film, with N_1 and N_2 representing the forces per unit length in the deformed geometry and H being the initial thickness of the film. The difference between σ_1 and $N_1 = H$ is caused by the significant change of the thickness of the film after deformation. This is also true for σ_2 and $N_2 = H$. Similar to the stretch ratios, the maximum stresses occur at $r = 0$, indicating that the centre of the film is the critical point governing the instability.

Electromechanical Instability

To evaluate the instability behaviour of the film under electromechanical loads, the relation between the initial stretch ratio (λ_0) and the maximum stretch ratio at the centre of the film (λ_m) is studied for different loading levels. For an applied pure pressure, this relation is depicted in figure 11 for the case where the thickness of the film is $H = 1mm$. The corresponding result for the case where an additional electric load with $q = 500pa$ applied is shown in figure 12. The figures show that for a specific initial stretch ratio, λ_0, if the applied pressure is too high then no corresponding λ_m can be determined, i.e. no solution can be found. Therefore, for any given initial stretch ratio, there exists a critical pressure at which the film will become unstable. This critical point can be determined by the maximum of the $\lambda_0 - \lambda_m$ curve. The comparison between figures 11 and 12 show that the applied electric field significantly changes the position of the maximum and, therefore, affects the instability of the film.

The critical pressure for different initial stretch ratios for this film is depicted in figure 13 for different electric voltages to show the critical loading conditions at which the film will become unstable. It can be observed that the applied electric field significantly reduces the level of the critical pressure.

Multi-mode Deformation of the Films

Another important and interesting phenomenon in the large deformation of dielectric elastomer films is the existence of multiple deformation modes.

From figures 11 and 12 it can be seen that for a given initial stretch ratio λ_0, if the applied pressure is low enough, it is possible to find two different λ_m, indicating that there exist at least two different deformations for the applied pressure. In fact, more than two deformation modes can be found under some loading conditions. To clearly explain this phenomenon, the relation between the initial stretch ratio λ_0 and the maximum stretch ratio in the film λ_m is depicted in figure 14 for λ_m with values up to 40 for an applied pressure $p = 3000pa$. If an initial stretch ratio $\lambda_0 = 1.2$ is applied, at least three different λ_m values, i.e. three solutions, can be determined. The profiles of the film under these three deformation modes are depicted in figure 15 with modes 1, 2 and 3 representing the modes from the low λ_m value to the high λ_m value. Figure 16 shows the multiple deformation of the film when an electric voltage and a pressure are applied with $Q = 1000pa$ and $p = 3000pa$. The initial stretch is assumed to be 1.4. The second and third modes are quite similar when both the pressure and the electric voltage are applied.

5. CONCLUSIONS

A theoretical study is provided to evaluate the nonlinear behaviour of a circular dielectric elastomer film subjected to an applied pressure and an electric voltage across the electrodes attached to its two surfaces and a pressure load. Nonlinear differential equations are established based on the deformed geometry, which includes the large rotation of the film. Numerical simulation is conducted by using an iteration process to study the effect of the geometry, the pre-strain and the applied loads upon the large deformation of the film. The results indicate that the pre-stretch ratio of the film, the applied electric voltage and the applied pressure all have significant effect on the deformation of the film. The film will become unstable when a critical condition is reached, which is determined by the pre-strain and

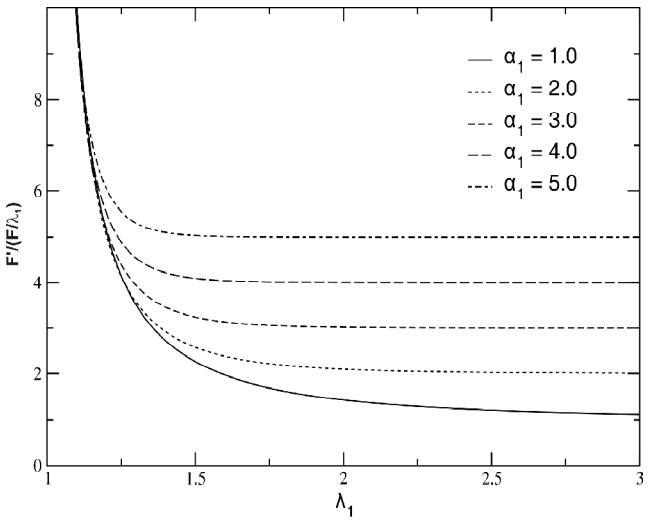

Figure 2: The Characteristic Function for Films Subjected to a Voltage and Inplane Forces

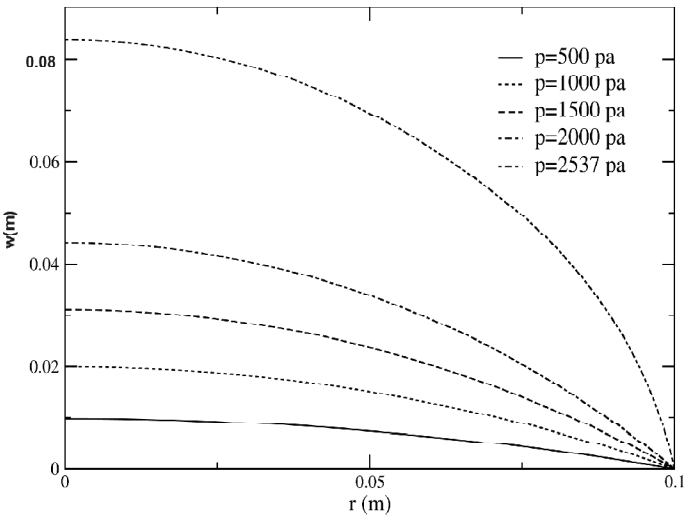

Figure 3: The Deflection of Films under an Applied Pressure

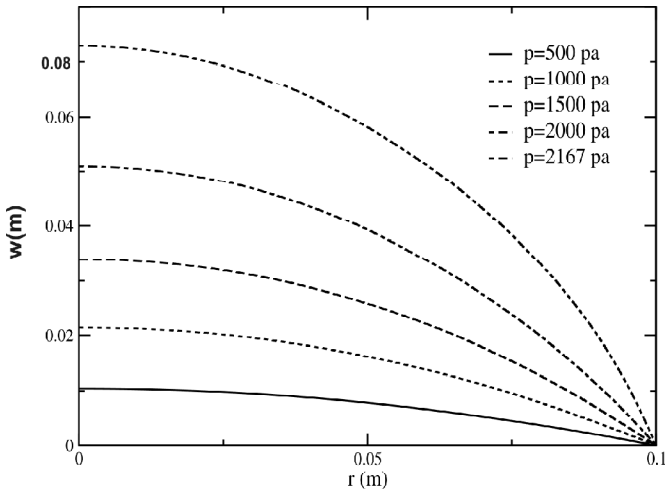

Figure 4: The Deflection of Films under Electromechanical Loads

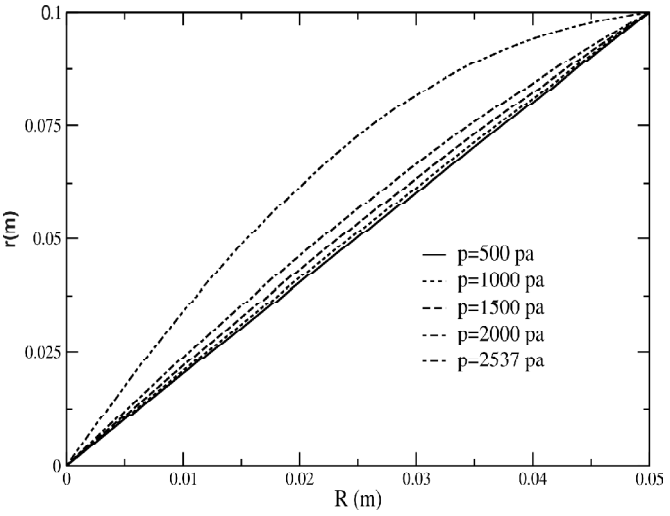

Figure 5: The Radial Deformation of Films under an Applied Pressure

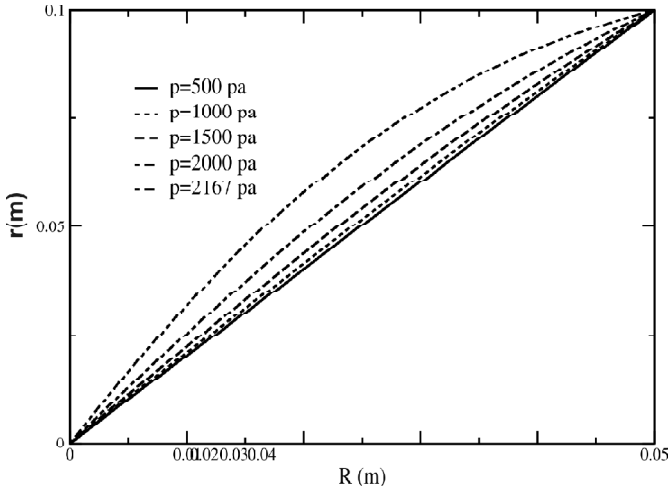

Figure 6: The Radial Deformation of Films under Electromechanical Loads

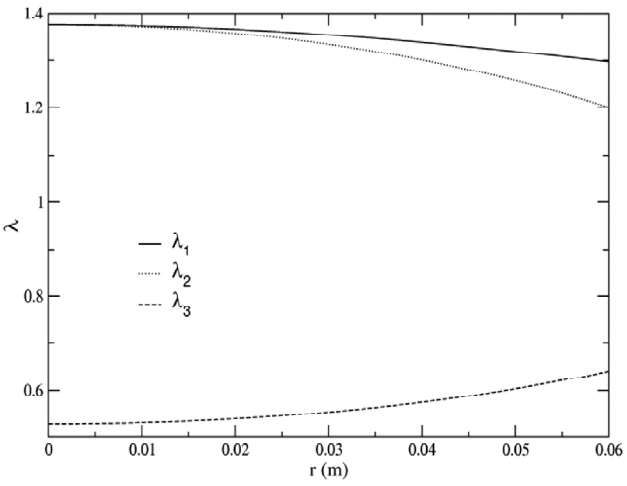

Figure 7: The Distribution of Stretch Ratios in Films under an Applied Pressure

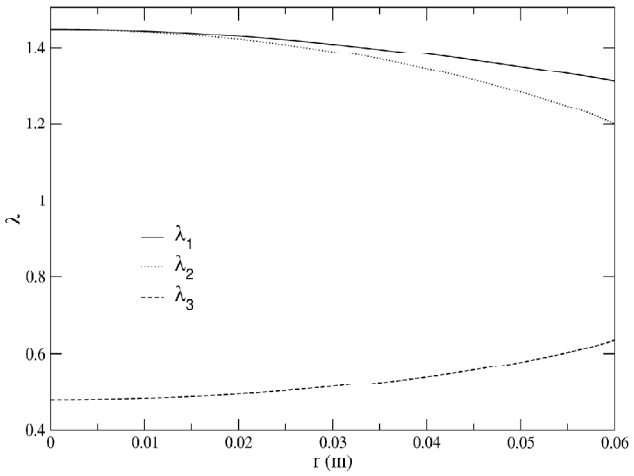

Figure 8: The Distribution of Stretch Ratios in Films under Electromechanical Loads

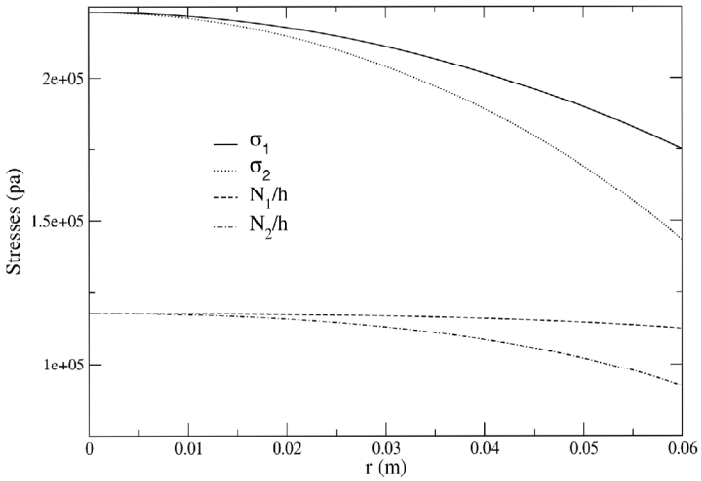

Figure 9: The Distribution of Stresses and Forces in Films under an Applied Pressure

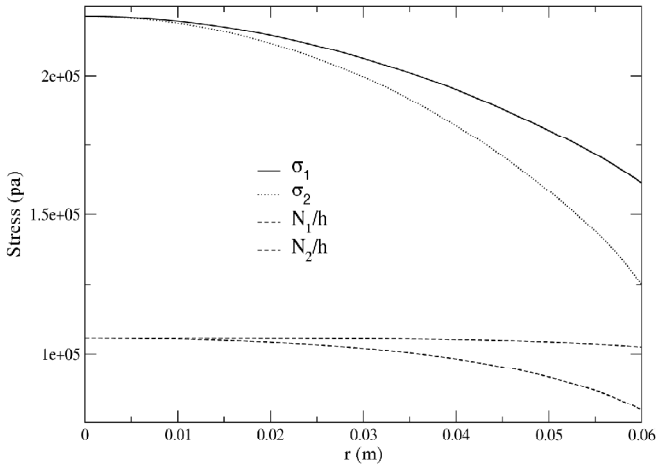

Figure 10: The Distribution of Stresses and Forces in Films under Electrome-chanical Loads

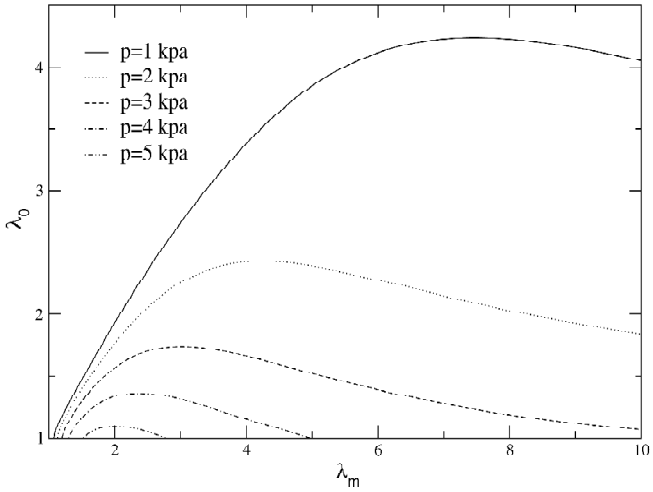

Figure 11: The Variation of Initial Stretch Ratio with the Maximum Stretch Ratio in Films Subjected to an Applied Pressure

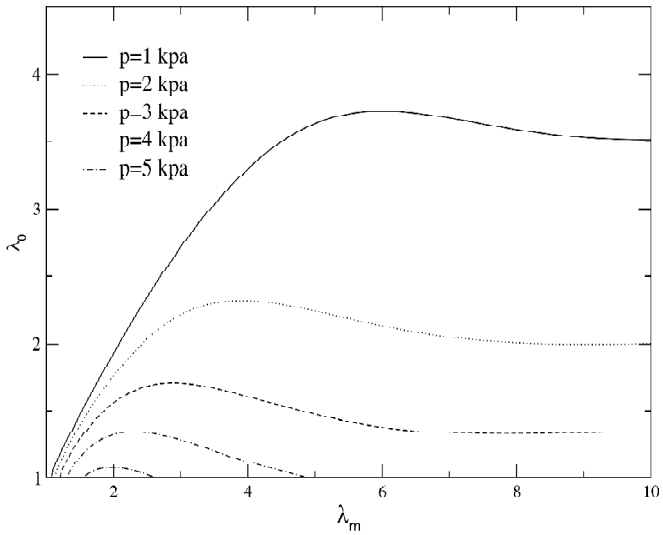

Figure 12: The Variation of Initial Stretch Ratio with the Maximum Stretch Ratio in Films Subjected to Electromechanical Loads

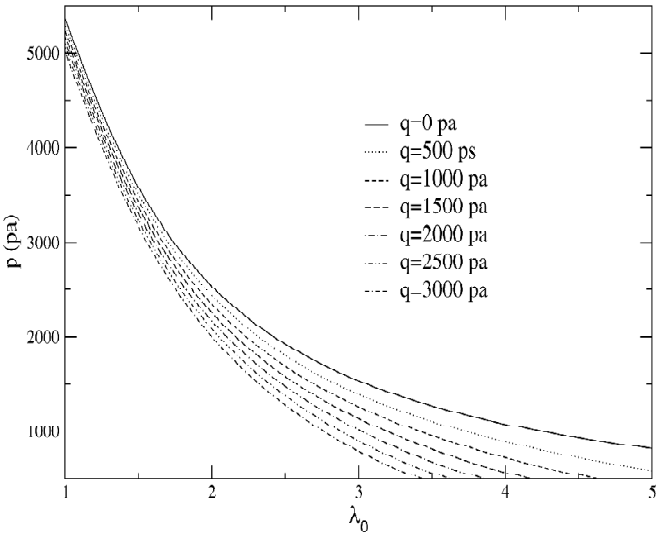

Figure 13: Critical Conditions for the Instable Deformation of Films

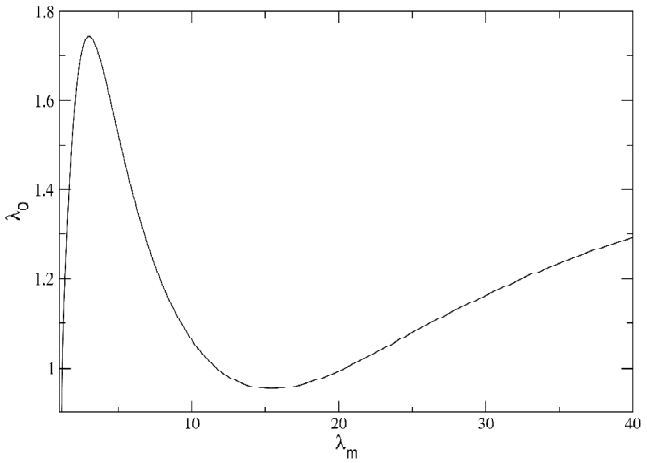

Figure 14: The Variation of Initial Stretch Ratio with the Maximum Stretch Ratio in Films Showing three Deformation Modes

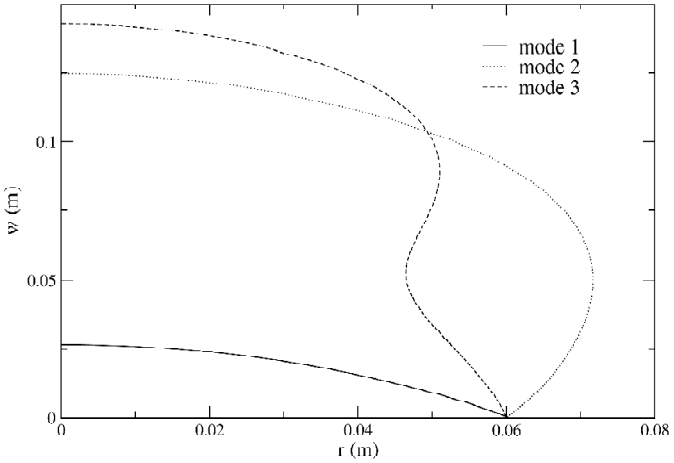

Figure 15: The Multiple Deformation Modes of Films Subjected to an Applied Pressure

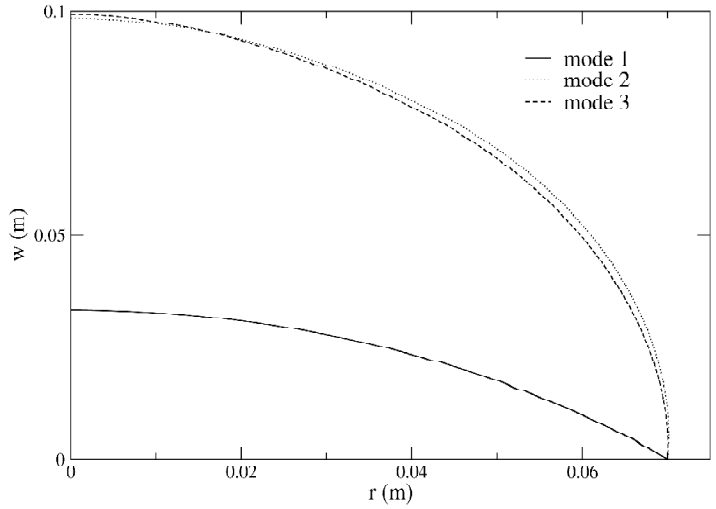

Figure 16: The Multiple Deformation Modes of Films Subjected to Electrome-chanical Loads

the applied voltage and pressure. In some loading cases, more than one solution may occur, resulting in multiple deformation modes of the film. The existence of the instability of the film and the multiple deformation modes indicates that in the design of electromechanical systems containing large deformation, detailed theoretical and experimental studies are necessary to fully understand the nonlinear behaviour of the systems.

Acknowledgements

This work was supported by the Natural Sciences and Engineering Research Council of Canada.

References

[1] Adkins, J. E. and Rivlin, R. S. (1952), Large Elastic Deformations of Isotropic Materials. IX. The Deformation of thin Shells. *Philosophical Transactions of the Royal Society of London*. Series A, 244, 505-531.

[2] Anderson, R. A. (1986), Mechanical Stress in a Dielectric Solid from a Uniform Electric Field. *Physical Review B*, 33, 1302-1307.

[3] Duan, H., Hu, Z. W. and Fang, Z. C. (2004), Study of Deformation Characters of a Large Rubber Circular Plate. *Modeling and Simulation in Materials Science and Engineering*, 12, 245-253.

[4] Giurgiutiu, V. Zagrai, A., Bao, J. (2002), Embedded Active Sensors For In-Situ Structural Health Monitoring of Thin-Wall Structures. *ASME Journal of Pressure Vessel Technology*, 124, 134-145.

[5] Goulbourne, N., Mockensturn, E. and Frecker, M. (2005), A Nonlinear Model for Dielectric Elastomer Membranes. *ASME Journal of Applied Mechanics*, 72, 899-906.

[6] Jackson, J. D. (1962), *Classical electro-dynamics*, Wiley, New York.

[7] Komaragiri, U, Begley, M. R. and Simmonds, J. G. (2005), The Mechanical Response of Freestanding Circular Elastic Films under Point and Pressure Loads, *ASME Journal of Applied Mechanics*, 72, 203-212.

[8] Mooney, M. (1940), A Theory of Large Elastic Deformation. *J. Appl. Phys.*, 11, 582-592.

[9] Ogden, R. W. (1972), Large Deformation Isotropic Elasticity - on the Correction of Theory and Experiment for Incompressible Rubberlike Solids. *Proc. Roy. Soc. London*, A326, 565-584.

[10] Parton, V. Z. Z. and Kudryavtsev, B. A. (1988), *Electromagnetoelasticity: Piezoelectrics and Electrically Conductive Solids*, Gordon and Breach Science Publishers, New York.

[11] Pelrine, R. E., Kornbluh, R. D. and Joseph, J. P. (1998), Electrostriction of Polymer Dielectrics with Compliant Electrodes as a Means of Actuation. *Sensors and Actuators*, A 64, 77-85.

[12] Pelrine, R., Kornbluh, R. and Kofod, G. (2000)(a), High-strain Actuator Materials based on Dielectric Elastomers. *Advanced Materials*, 12, 1223-1225.

[13] Pelrine, R., Kornbluh, R., Joseph, J., Heydt, R., Pei, Q. and Chiba, S., 2000(b), High-field Deformation of Elastromeric Dielectrics for Actuators. *Materials Science and Engineering*, 11, 89-100.

[14] Szyszkowski, W. and Glockner, P. G. (1984), Finite Deformation and Stability behaviour of Spherical Inflatables Subjected to Axi-symmetric Hydrostatic Loading. *International Journal of Solids and Structures*, 20, 1021-1036.

[15] Wang, X. D. (1999), Coupled Electromechanical Behaviour of Piezoelectric Actuators in Smart Structures. *Journal of Intelligent Material Systems and Structures*, 10, 232-241.

[16] Wang, X. D. and Meguid, S. A. (2000), On the Electroelastic Behaviour of a thin Piezoelectric Actuator Attached to an Infinite Host Structure. *International Journal of Solids and Structures*, 37, 3231-3251.

[17] Wissler, M. and Mazza E. (2005), Modeling of a Pre-strained Circular Actuator Made of Dielectric Elastomers. *Sensors and Actuators*, 120, 184-192.

[18] Wolfson, R. and Pasachoff, J. M. (1999), *Physics for Scientists and Engineers*, Addison-Weslay, Reading.

[19] Yeoh, O. H. (1993), Some Forms of the Strain Energy Function for Rubber. *Rubber Chem. Technol.*, 66, 754-771.

[20] Zhang, X., Lowe, C., Wissler, M., Jahne, B. and Kovacs, G. (2005), Dielectric Elastomers in Actuator Technology. *Advanced Engineering Materials*, 7, 361-367.